Annual Review of Control, Robotics, and Autonomous Systems

Robot Model Identification and Learning: A Modern Perspective

Taeyoon Lee,[1] Jaewoon Kwon,[1] Patrick M. Wensing,[2] and Frank C. Park[3]

[1]Naver Labs, Seongnam, South Korea; email: ty-lee@naverlabs.com, jaewoon.kwon@naverlabs.com

[2]Department of Aerospace and Mechanical Engineering, University of Notre Dame, Notre Dame, Indiana, USA; email: pwensing@nd.edu

[3]Department of Mechanical Engineering, Seoul National University, Seoul, South Korea; email: fcp@snu.ac.kr

Annu. Rev. Control Robot. Auton. Syst. 2024. 7:311–34

First published as a Review in Advance on October 20, 2023

The *Annual Review of Control, Robotics, and Autonomous Systems* is online at control.annualreviews.org

https://doi.org/10.1146/annurev-control-061523-102310

Keywords

system identification, model learning, geometry, inductive bias

Abstract

In recent years, the increasing complexity and safety-critical nature of robotic tasks have highlighted the importance of accurate and reliable robot models. This trend has led to a growing belief that, given enough data, traditional physics-based robot models can be replaced by appropriately trained deep networks or their variants. Simultaneously, there has been a renewed interest in physics-based simulation, fueled by the widespread use of simulators to train reinforcement learning algorithms in the sim-to-real paradigm. The primary objective of this review is to present a unified perspective on the process of determining robot models from data, commonly known as system identification or model learning in different subfields. The review aims to illuminate the key challenges encountered and highlight recent advancements in system identification for robotics. Specifically, we focus on recent breakthroughs that leverage the geometry of the identification problem and incorporate physics-based knowledge beyond mere first-principles model parameterizations. Through these efforts, we strive to provide a contemporary outlook on this problem, bridging classical findings with the latest progress in the field.

1. INTRODUCTION

In recent years, the field of robotics has witnessed a significant increase in the complexity and importance of safety in robotic tasks. Notable examples include legged robots capable of running and performing highly athletic motions, as well as manipulators and multifingered hands executing dexterous, nonprehensile manipulation tasks. The growing complexity of these tasks has highlighted the necessity for accurate and dependable robot models.

Traditionally, physics-based dynamic models have been the go-to approach for approximating the input–output behavior of robots. These models rely on principles derived from classical mechanics to describe the robot's motion and interaction with the environment. Recently, pure data-driven approaches (e.g., from machine learning) have gained momentum because they offer the possibility of learning robot models directly from data without explicitly modeling the underlying physics. These approaches aim to reconstruct input–output behavior based solely on observed data, leveraging the power of statistical learning techniques. This shift toward pure data-driven models has sparked a discussion about their potential to augment or even replace traditional physics-based models in certain contexts.

In fact, the problem of approximating the input–output behavior of a system from data, referred to as the system identification or model learning problem, has a long history in robotics. Earlier approaches to robot model identification aimed to improve the accuracy of the physical parameters of physics-based models by collecting joint kinematics and torque data. After all, the availability, coverage, and quality of the data samples play a central role in accurately approximating reality in both physics-based and physics-free approaches. Unfortunately, acquiring extensive and sufficiently rich data from real robotic systems can be challenging, particularly for complex systems and when safety concerns arise. Even for mechanics-based models, identifying a minimal set of parameters that represents the rigid-body dynamics of a standard humanoid structure (often requiring hundreds of parameters) becomes highly challenging, particularly in terms of generalizing the model predictions across unforeseen initial states and system inputs.

One of the primary objectives of this review is to provide a unified perspective on the system identification problem across the robotics and machine learning literature. It aims to shed light on the challenges encountered in identifying accurate and reliable models for different types of robots, as well as the recent advancements in system identification within the robotics domain. The intended audience comprises individuals with a background in machine learning who seek to comprehend the challenges and recent advances in system identification for robotics, as well as those with a background in robotics who are interested in the recent progress of methods that go beyond mechanics-based parameterizations for modeling physical systems.

Of course, this article does not aim to provide an exhaustive review of all system identification and model learning methods. Rather, it focuses on recent advances that aim more to incorporate domain-specific (physics-based) knowledge in order to develop sample-efficient and robust methods that go beyond classical parameterizations, yet without treating system identification as a complete black-box function approximation problem. By doing so, it aims to provide a modern perspective on the problem.

The remainder of the article is structured as follows. Section 2 provides background on the problem of model learning for nonlinear systems, emphasizing a general viewpoint on the problem often adopted in the machine learning literature. We use this section to motivate the main challenges facing dynamic modeling and identification and then, in Section 3, detail the more specific structure of the problem for robot model identification. We concentrate on the classical problem of identifying inertial parameters of a mechanism, and in Section 4 we describe recent advances that leverage the geometric structure of rigid-body inertial parameters to improve the efficiency and learning of dynamic models. Section 5 then moves beyond this classical setting

and discusses more recent paradigms that are physics informed, while offering more model-form flexibility. Section 6 concludes the article.

2. BACKGROUND ON DYNAMIC MODEL IDENTIFICATION AND LEARNING

In this section, we provide a brief overview of the essential procedures and challenges for general nonlinear system identification problems, with the primary aim of bridging approaches to system identification in robotics and model learning in machine learning.

Consider the true state-space nonlinear system dynamics of the form

$$\begin{aligned} x_{t+1} &= f(x_t, u_t, \omega_t), \\ y_t &= h(x_t, u_t, \epsilon_t), \end{aligned} \qquad 1.$$

where $x_t \in \mathcal{X} \subseteq \mathbb{R}^n$ is the state, $u_t \in \mathcal{U}$ is the control input, $\omega_t \in \mathcal{W}$ is the process noise, and $y_t \in \mathcal{Y}$ is the output measurement, with $\epsilon_t \in \mathcal{E}$ being the measurement noise. The system identification problem typically begins by selecting the set of model candidates, which is assumed to include within it the true system dynamics. Let us consider parametric model classes $\mathcal{M}_f = \{f_\theta : \mathcal{X} \times \mathcal{U} \times \mathcal{W} \to \mathcal{X} \,|\, \theta \in \Theta\}$ and $\mathcal{M}_h = \{h_\theta : \mathcal{X} \times \mathcal{U} \times \mathcal{E} \to \mathcal{Y} \,|\, \theta \in \Theta\}$, where a particular instantiation of the system dynamics with parameter θ is given by[1]

$$\begin{aligned} x_{t+1} &= f_\theta(x_t, u_t, \omega_t), \\ y_t &= h_\theta(x_t, u_t, \epsilon_t). \end{aligned} \qquad 2.$$

By executing a series of control inputs $u_1, \ldots, u_N$, one collects a finite number of data samples, $\mathcal{D} = \{u_1, y_1, \ldots, u_N, y_N\}$, from the true system in the real world. Then, the goal is to find the model parameter vector θ that best matches the input–output behavior of the true system dictated by the collected data and the selected model class $\mathcal{M}$. For this, it is essential to define an error criterion to be optimized between the true system and the model based on the finite number of data samples. Such a criterion should provide a statistically meaningful objective and/or be informed by the specific usage of the identified model in practice. It is worth noting that, in reality, this process is often not a one-shot ordeal. During validation of the identified model, deficiencies can be exposed due to multiple factors, such as the choice of model class $\mathcal{M}$, the quality and sufficiency of the data samples, the choice of error criterion, or even the parameter estimation algorithms employed.

2.1. Parameter Identifiability (It Matters . . . or Does It?)

The concept of structural identifiability asks the question of whether different model instances within the model class uniquely represent different input–output behaviors. More formally, a particular parameterized model class is said to be structurally identifiable if the parameters can be uniquely determined from the input–output behavior—i.e., if $y(\theta_1) \equiv y(\theta_2)$ for all inputs, then $\theta_1 = \theta_2$. This property naturally leads to the uniqueness and existence of the solution θ to the identification problem, but with the conditions that the true system is within the specified model class and an infinite amount of data that covers all cases is available. Given that the amount of data

[1]The present description of the model is often called a gray-box model in the nonlinear control systems literature (1); for a more general, comprehensive treatment of nonlinear system models and the associated identification problem, we direct readers to Reference 2. We also note that the collection of state variables x_t or their representation within the dynamics model may not generally be identical to the one for the true system; for example, one may choose to neglect the effect of thermodynamics or aerodynamics when modeling the rigid-body dynamics of a robot manipulator. The state representation itself can also be auxiliary and learned from data, which is common in learning-based approaches with camera images as outputs (3).

collectible from robots is always finite, a more viable description of identifiability to practitioners may be described by accounting for the statistical precision of the parameter estimates. Practically identifiable parameters for a given dataset can be considered to be ones with confidence intervals smaller than some threshold.

Meanwhile, the concept of parameter identifiability pertains to a parameter-centric view of the model identification process: How accurately do the estimated parameters $\hat{\theta}$ revealed from data match the true values? This aspect is less relevant with data-driven learning using black-box models such as deep neural network models, since parameters therein are not interpretable and do not often provide a unique construction of input–output behavior. On the other hand, parameters within mechanics-based models, such as mass, inertia, and stiffness, have tangible and physical meanings that analytically relate to the global description of physical behaviors of a system.

Above all, system identification is all about the statistical approximation of the input–output behavior of a system. Then, how can we systematically integrate our understanding of physical parameters into statistical parameter identification of mechanics-based models for improved robustness? Further, how can we construct an extended class of parameterized models that globally relate to our understanding of physical behaviors of robotic systems? We continue our discussion of these matters later (Sections 4 and 5) and next present generic formulations of the data-driven model identification problem and sources of errors in the identification process.

2.2. On the Choice of Error Criterion

Employing statistical motivations to construct the error criterion is common in system identification. One can define a joint probability density function for the output data samples, $p_\theta(y_{1:N}|u_{1:N})$, induced from the stochastic nonlinear dynamics model in Equation 2.[2] Then, the maximum likelihood estimation (MLE) formulation for approximating θ can be written as minimizing the negative log-likelihood function $L(\theta)$, i.e.,

$$L(\theta) = -\log p_\theta(y_{1:N}|u_{1:N}). \tag{3.}$$

While the joint probability density function is, in general, computationally intractable, the incorporation of practically viable structure in the model allows computationally tractable algorithms for estimating θ in practice. For instance, let us consider the case of a noise-free full-state measurement model, i.e., $x_{t+1} = f_\theta(x_t, u_t, \omega_t)$, $y_t = x_t$. Then, the MLE objective can be decomposed as follows:

$$L(\theta) = -\sum_{t=1}^{N} \log p_\theta(x_t|x_{t-1}, u_{t-1}), \tag{4.}$$

where the probability density function $p_\theta(x_t|x_{t-1}, u_{t-1})$ can now be solely defined by the dynamic model (Equation 2). A different likelihood function (given that x_{t+1} and ω_t are one-to-one for every fixed x_t, u_t) can be considered to be[3]

$$L(\theta) = -\sum_{t=1}^{N} \log p(\omega_t), \quad \text{such that} \quad x_{t+1} = f_\theta(x_t, u_t, \omega_t) \quad \text{for} \quad t = 0, \ldots, N-1. \tag{5.}$$

[2]Here, we omit the dependence of the joint probability density with respect to the initial state x_0 and assume it is given.

[3]The objective in Equation 5 is, in general, different from that in Equation 4, since $\log p_\theta(x_{t+1}|x_t, u_t) = \log p(\omega_t) - \log\det(\partial x_{t+1}/\partial \omega_t)$. However, if $\partial x_{t+1}/\partial \omega_t$ is constant, e.g., $x_{t+1} = f_\theta(x_t, u_t) + \omega_t$, then they are identical.

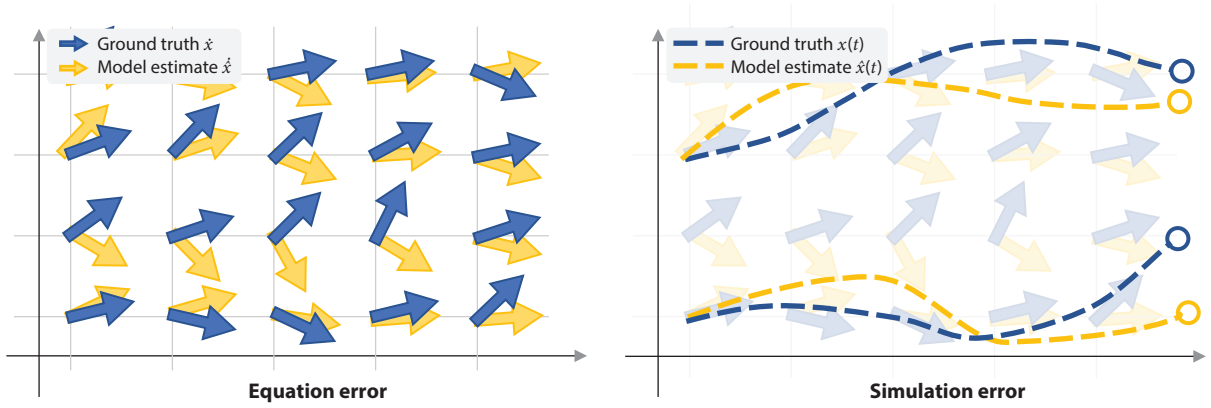

Figure 1

Equation error criteria versus simulation error criteria. Equation error criteria consider the error in a one-step prediction, while simulation error criteria consider the accumulation of model mismatch over trajectories or multistep predictions. From a continuous-time view, the equation error criteria correspond to the difference between the vector fields of the dynamic models, while the simulation error is calculated based on the difference between their integral curves.

These types of formulations are commonly referred to as employing an equation error or one-step-ahead prediction error criterion (see **Figure 1**). Loosely speaking, the parameters are optimized to fit the average error in the local state transition dynamics.

On the other hand, another class of error criteria that deserves attention is the so-called simulation error criterion (see **Figure 1**), which aims at minimizing the deviation between the measured outputs and the ones simulated or integrated using the model (4–6). To illustrate, the simulation error criterion can typically be given in the form

$$L(\theta) = \sum_{i=1}^{N} \|\hat{x}_i - x_s(i, \theta)\|^2, \qquad 6.$$

where $\hat{x}_i$ is the state measurement and $x_s(i, \theta)$ is the ith-step-ahead prediction of the state by simulating with the model, i.e., $x_s(i, \theta) = f_\theta(x_s(i-1, \theta), u_{i-1})$ for $i = 1, \ldots, N$, with $x_s(0, \theta) = x_0$. It should be noted that the simulation error also admits the maximum likelihood interpretation under full-state measurement with white Gaussian noise and noise-free state dynamics, i.e., $x_{t+1} = f(x_t, u_t)$, $y_t = \hat{x}_t = x_t + \epsilon_t$, where $\epsilon_t \sim \mathcal{N}(0, \sigma^2 I)$. More generally, an output error criterion can be defined as minimizing the simulated error on the output, i.e., $L(\theta) = \sum_{i=1}^{N} \|y_i - h_\theta(x_s(i, \theta))\|^2$.

Without statistical grounding, the simulation error criterion is inherently different from the equation error criterion in that it reflects the parametric estimation error more globally, rather than locally, by directly integrating the system dynamics model over time. In that regard, the simulation error criterion better exposes the nature of the system identification problem in that it is not simply a static estimation problem but involves dynamics that relate to the sequential input–output behavior of the system. Some errors in the parameters that contribute to minor effects in the equation error can lead to severe deviation from the true system dynamics over time. For instance, consider a simple one-dimensional mass–damper system, $m\ddot{q} + d\dot{q} = 0$, where m is the mass and d is the damping coefficient. While any possible bounded estimation error on the mass and damping coefficients only leads to bounded equation error, errors that lead to negative values in any of these parameters lead to an unstable forward simulation of the dynamics that can produce exponentially diverging simulation error over time [i.e., $\dot{q} = \dot{q}_0 \exp(-td/m)$]. For this reason,

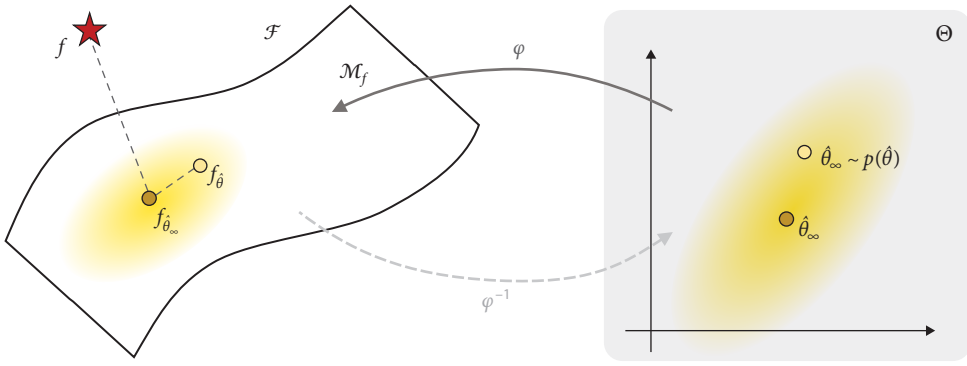

Figure 2

A conceptual picture of the source of errors. Through a mapping $\varphi : \Theta \to \mathcal{M}_f$, the parameter θ is related to the dynamic model, i.e., $f_{\hat{\theta}} = \varphi(\hat{\theta}) \in \mathcal{M}_f$. Its inverse mapping φ^{-1} exists only if the model is structurally identifiable. $\mathcal{F}$ represents the ambient space in which the model set $\mathcal{M}_f$ is embedded. The ground truth description of the system $f \in \mathcal{F}$ (denoted by the *red star*) is not necessarily within the model set. The yellow gradation represents the probability distribution $p(\hat{\theta})$ of the estimated parameters that is induced by the stochasticity of the finite data samples and the specific identification method employed, i.e., $\hat{\theta} = \mathrm{ID}(\mathcal{D})$, $\mathcal{D} \sim p(y_{1:N}|u_{1:N})$. Structural error persists even when the random error is resolved with an infinite number of samples, i.e., $f_{\hat{\theta}_\infty} \in \mathcal{M}_f$.

minimizing simulation errors is generally more appealing to increase the simulation fidelity or for use in receding-horizon predictive control or model-based reinforcement learning. However, compared with equation error approaches, this method is usually highly computationally demanding, requiring iterative simulation of the model in the computation loop, and is subject to a nonconvex optimization landscape, which may not be suitable for, e.g., online identification or adaptive control.

2.3. Source of Errors

Suppose that the true system dynamics is within the model candidate set, i.e., that there exists $\bar{\theta} \in \Theta$ such that $f = f_{\bar{\theta}} \in \mathcal{M}_f$. Then, as the sample size tends to infinity and remains complete [i.e., $L(\theta)$ has a unique global minimum], the maximum likelihood estimate of θ is known to converge to $\bar{\theta}$. In such a case, the estimator is said to be statistically consistent. However, these assumptions rarely hold true in practice because (*a*) modeling can almost always be inaccurate to some degree (i.e., introducing structural error), (*b*) the data can be noisy (i.e., introducing random error), and (*c*) the data can be incomplete. Below, we discuss how these problems manifest more specifically; **Figure 2** provides a conceptual picture of the source of errors.

2.3.1. Structural error. In scenarios where the problem of model mismatch (i.e., $f \notin \mathcal{M}_f$) is prevalent, the conventional approach of conducting statistical analysis on parameter estimation performance tends to be less viable. Even when abundant and comprehensive data samples are available, uncorrectable biases in the model structure can corrupt parameter estimates in unpredictable ways.

There are many components in real robotic systems that are difficult to model accurately using standard mechanics-based models. For instance, complex frictions involving stick, slip, and state dependency; nonlinear hysteresis; and slackening effects from tendon-driven mechanisms (7), as well as cascaded actuator dynamics (8), are among the components that standard mechanics-based models struggle to describe with sufficient accuracy.

Also, it should be emphasized that the problem of model mismatch may arise not only from factors related to difficult-to-model effects. If the fixed parameters in a physical model actually contain significant errors, failure to identify them along with other parameters may lead to structural bias issues. For instance, as noted by Kwon et al. (9), kinematic parameter error in the dynamics model can cause significant structural bias in estimating dynamic parameters.

2.3.2. Data: randomness and incompleteness. Random error refers to the estimation error or variance that is incurred by the stochasticity in the system dynamics or noise in the output measurements. Apart from structural error, random error can, in principle, be resolved by having a sufficient amount of and complete measurement data.

Then, given a diverse and complete sampling, one should be able to determine how many data samples are needed to ensure a practically reliable estimation of the model parameters. The Fisher information matrix is given as

$$\mathcal{I}(\bar{\theta}, u_{1:N}) = \mathbb{E}_{p_{\bar{\theta}}}\left[\nabla_\theta \log p_\theta(y_{1:N}|u_{1:N}) \cdot \nabla_\theta \log p_\theta(y_{1:N}|u_{1:N})^{\mathrm{T}} \,|\, \bar{\theta}\right], \qquad 7.$$

which measures the amount of information that data samples carry about the unknown true parameter vector $\bar{\theta}$. Importantly, this definition relates to the Cramer–Rao bound, which sets the theoretically achievable estimation covariance of the parameters, i.e., $\mathrm{var}[\hat{\theta}] \succeq \mathcal{I}(\bar{\theta})^{-1}$, when $\hat{\theta}$ denotes an arbitrary unbiased estimator for θ. Accordingly, this measure is commonly used to discern a practically identifiable parameter set from data or (as noted in the sidebar titled The Data Collection Problem) to guide the design of an optimal data collection strategy before identification. Herein, we refer to data being incomplete in the case where the information matrix $\mathcal{I}(\theta)$ (conditioned on the specific data collection experiment $u_{1:N}$) is degenerate along certain subspaces within the structurally identifiable parameter space, i.e., $\delta^{\mathrm{T}}\mathcal{I}(\theta)\delta \equiv 0$ for $\delta \neq 0, \delta \in \mathbb{R}^{\dim(\Theta)}$. For example, when data are collected from static postures of a robot, they inherently lack complete information concerning the robot's inertial properties, irrespective of their structural identifiability.

THE DATA COLLECTION PROBLEM

The fact that the information matrix offers a measure of how the data samples impact the parameter estimation performance makes it possible to optimize the data collection strategy, which is known as optimal experimental design or the optimal excitation problem (5, 10), i.e.,

$$\max_{u_{1:N}} \ \sigma\big(\mathcal{I}(\bar{\theta}, u_{1:N})\big). \qquad \text{SB1.}$$

An intricate issue regarding constructing a physically meaningful scalar measure $\sigma : \mathbb{R}^{\dim(\Theta)\times\dim(\Theta)\to\mathbb{R}}$ out of the matrix-valued information measure $\mathcal{I}(\bar{\theta})$ is discussed in Section 4.4. The information matrix is in general dependent on the unknown parameter $\bar{\theta}$, which, in practice, typically requires nominal values of θ to proceed with optimization. We note that there are also experimental design criteria that are based on the output prediction error variance (11), as opposed to parameter error variance, essentially by projecting the influence of parametric error to some distribution of output predictions.

Meanwhile, it is worth noting that solving data collection problems in order to identify unknown parameters is somewhat akin to a chicken-and-egg problem in general robotics applications. Specifically, while we require trajectory data samples that excite the full spectrum of the dynamics to obtain a good model estimate, designing and executing dynamic motions safely without an accurate dynamics model can be challenging. Consequently, optimal excitation of robot motions has been studied mainly on fixed-base, fully actuated robots, such as robot manipulators (5), which are less safety critical than floating-base, underactuated robots, such as humanoids (12). Considering safety in high-performance control under model uncertainty is itself an important and active area of research (for a recent review, see 13).

3. SYSTEMS AND METHODS IN ROBOT MODEL IDENTIFICATION

In this section, we review methods in robot dynamic identification that are based on traditional mechanics-based models, with a particular focus on rigid-link robots; interested readers may also consult a recent review on soft robot modeling (14). The main focus of this review is to highlight how generic identification formulations give rise to specific challenges for the identification of robotic systems, taking into account their unique characteristics and different applications. It is important to note that the recent insights and advancements in robot dynamic identification methods presented in Sections 4 and 5 are not mutually exclusive to the ones reviewed here but rather complement them.

3.1. Systems without Contact or with Contact Force Measurements

We begin by examining identification methods applicable to systems either free of external contacts or, in cases where such contacts are present, involving contact force measurements.

3.1.1. Fixed-base systems. The seminal work by Atkeson et al. (15) led to a popular linear least-squares objective for robot dynamic model identification, which follows the equation error formulation (Equation 5). Their key contribution recognized that the mass–inertial parameters ϕ (Equation 12) of robot links and loads appear linearly in the inverse dynamics equation of rigid-body systems. To illustrate, for an N_L-link fixed-based robot manipulator with joint configuration variables $q \in \mathbb{R}^n$ and a joint input torque vector $u \in \mathbb{R}^n$ with additive Gaussian noise ω, i.e., $w \sim \mathcal{N}(0, \Sigma)$, the second-order inverse dynamics equation can be described as

$$u + \omega = M(q, \psi)\ddot{q} + b(q, \dot{q}, \psi) \equiv Y(q, \dot{q}, \ddot{q})\psi, \qquad 8.$$

where $M(q, \psi) \in \mathbb{R}^{n \times n}$ is the mass matrix, $b(q, \dot{q}, \psi) \in \mathbb{R}^n$ denotes the vector of Coriolis and gravitational forces, and $\psi = [\phi_1, \ldots, \phi_{N_L}]$ denotes the complete set of mass and inertial parameters of each of the links (and also typically includes joint Coulomb and viscous friction parameters). A structurally identifiable set of parameters (see the sidebar titled Structurally Identifiable Parameters of Rigid-Body Dynamic Models) linearly lumps together parameters in ψ (i.e., via $\theta = B\psi$), and the terms in Equation 8 can be collected and represented in the most compact form as (16)

$$u + \omega = M(q, \theta)\ddot{q} + b(q, \dot{q}, \theta) \equiv \Gamma(q, \dot{q}, \ddot{q})\theta, \qquad 9.$$

where $\Gamma(q, \dot{q}, \ddot{q}) \equiv Y(q, \dot{q}, \ddot{q})B$. Then, given the measurements of states $y = x = (q, \dot{q})$ and $\ddot{q}$ (through appropriate numerical differentiation and filtering) at multiple points $t = 1, \ldots, N$ along some reference trajectory, the negative log-likelihood objective can be given as $L(\theta) = \sum_{i=1}^{N} -\log p(\omega_i) \sim \sum_{i=1}^{N} \|\Gamma(q_i, \dot{q}_i, \ddot{q}_i)\theta - u\|^2_{\Sigma^{-1}}$ (see Equation 5).

Such an inherent linear-in-parameters property for the robot dynamics equation has prompted the adoption of a rich class of robust identification techniques that rely on linear models. Many of these approaches relax the noise-free assumptions on the regressor matrix (22) and the statistical independence assumption between the regressor matrix $\Gamma(q, \dot{q}, \ddot{q})$ and the input u (5, 23), impose a non-Gaussian distribution on ω to derive robust linear regression methods (24), or employ set membership uncertainty to estimate the acceptable parameter error bound within, e.g., robust control (25). To some extent, all of these methods are concerned with fitting the equation error that represents the local error of the dynamics.

There have also been methods that explore the use of simulation/output error criteria (4) or composite ones (e.g., approximating the simulation error solution in a computationally efficient way using an equation error formulation) (6) in the identification of robot manipulators

STRUCTURALLY IDENTIFIABLE PARAMETERS OF RIGID-BODY DYNAMIC MODELS

Multibody dynamics models of the form $u + w = Y(q, \dot{q}, \ddot{q})\psi$ are not structurally identifiable when ψ contains the 10 standard inertial parameters of each body (17). This property is due to the fact that each connecting joint creates ambiguity in how mass or inertia can be assigned to links on either side of the joint without affecting the dynamics (16). Formally, the ambiguity can be characterized via the set

$$\mathcal{N} = \{\delta | Y(q, \dot{q}, \ddot{q})\delta = 0, \forall q, \dot{q}, \ddot{q}\}.$$

If $\overline{\psi}$ denotes the true parameters, then any ψ in the affine subspace $\overline{\psi} + \mathcal{N}$ gives the same dynamic model and measurements. To recover structural identifiability, a reparameterization is often pursued using so-called base parameters, denoted as θ. This task can be accomplished by choosing a basis for $\mathcal{N}^{\perp}$ (the orthogonal complement of $\mathcal{N}$) as follows. Suppose we have a fixed full-rank matrix B such that $\text{Range}(B^{\mathrm{T}}) = \mathcal{N}^{\perp}$. Then, for this selection, $\theta_i = \sum_j B_{ij}\psi_j$ gives the ith base parameter as an identifiable linear combination of the standard parameters ψ_j. While $\mathcal{N}^{\perp}$ is unique, the choice of B, and thus the choice of base parameters, is not. B can be chosen in row-reduced echelon form (or similar) so that each base parameter represents a regrouping (18) into a standard parameter, which can be desirable for efficient simulation (19).

Many methods exist to reparameterize a model with base parameters. Base parameter sets can be constructed using symbolic methods via the analysis of the dynamics equations (17, 18, 20), numerically via QR or singular value decompositions applied to regressors of assumed maximally exciting data (21), or geometrically by recursively characterizing how each link is able to be excited (16). Many symbolic methods do not guarantee that the resulting reparameterization is structurally identifiable except in special cases, while numerical methods will underestimate the number of base parameters if the data used are not fully exciting.

and have been proven to result in more robust identification results compared with ones that are based purely on equation error. These methods are usually performed using a closed-loop dynamics simulation [i.e., proportional–derivative (PD)–controlled manipulator dynamics with a reference trajectory signal as input] to enhance the stability of the forward simulation computation within identification (26). For a more comprehensive review on parameter identification of robot manipulators, we direct readers to Reference 27.

3.1.2. Floating-base systems. Floating-base systems like humanoid or quadruped robots are inherently underactuated; for these systems, the dimension of configuration space $q = (q_{\mathrm{j}}, q_{\mathrm{r}}) \in \mathbb{R}^{n+6}$ is larger than the number of input torque actuations $u \in \mathbb{R}^n$, where $q_{\mathrm{j}} \in \mathbb{R}^n$ denotes the joint configuration and $q_{\mathrm{r}} \in \mathbb{R}^6 \simeq \mathrm{SE}(3)$ represents the pose and orientation of a floating-base (root) link. The dynamics equation subject to (known) contact forces λ_i for $i = 1, \ldots, n_{\mathrm{c}}$ can be described as

$$\begin{bmatrix} u \\ 0 \end{bmatrix} + \sum_{i=1}^{n_{\mathrm{c}}} \begin{bmatrix} J^{\mathrm{c}}_{\mathrm{j},i}(q)^{\mathrm{T}} \\ J^{\mathrm{c}}_{\mathrm{r},i}(q)^{\mathrm{T}} \end{bmatrix} \lambda_i = M(q, \theta)\ddot{q} + b(q, \dot{q}, \theta) \equiv \begin{bmatrix} \Gamma_{\mathrm{j}}(q, \dot{q}, \ddot{q}) \\ \Gamma_{\mathrm{r}}(q, \dot{q}, \ddot{q}) \end{bmatrix} \theta, \qquad 10.$$

where $J^{\mathrm{c}}_i = [J^{\mathrm{c}}_{j,i}, J^{\mathrm{c}}_{r,i}]$ denotes the Jacobian of the contact points. As shown in the second block of Equation 10, one remarkable finding was that, in the case of open-chain rigid-body systems, the structurally identifiable set of parameters θ of the full dynamics equation can be equally identified solely from the base-link dynamics, i.e., $\sum_{i=1}^{n_{\mathrm{c}}} J^{\mathrm{c}}_{r,i}(q)^{\mathrm{T}}\lambda_i = \Gamma_{\mathrm{r}}(q, \dot{q}, \ddot{q})\theta$ (28). Identifying parameters without employing joint-space dynamics is particularly appealing for systems in which joint torque input is unobservable, such as human subjects (29), or when other structural errors, such as those

from joint friction models, can severely bias the parameter identification. However, the reduced nature of identification without joint torque measurements generally implies a challenge in that there is less information to be employed for accurately identifying the parameters in a way that generalizes to prediction with the full dynamic model. Not surprisingly, one study demonstrated that the identification using only contact force measurements generalized less accurately for predicting the joint space dynamics than the identification employing contact force and joint torque data (30).

A fundamental challenge within generic system identification of floating-base systems, as also noted in the sidebar titled The Data Collection Problem, is that collecting sufficiently rich, dynamic data is often unattainable compared with the case for, e.g., fixed-based robot manipulators. This can often lead to highly biased parameter estimates that are not physically consistent and are less generalizable for use within high-performance simulation and control (31). Constrained optimization approaches to guarantee physically consistent estimates (32–34) and regularized formulations to exploit the nominal parameter information (e.g., from CAD data) have been studied (35, 36). These methods were later reimagined and improved following the geometric perspective presented in Section 4.

3.2. Systems with Contact and without Contact Force Measurements

System identification under contact without contact force measurements remains challenging, in large part due to the nonsmooth and hybrid nature of the dynamics,

$$Bu + \sum_{i=1}^{n_c} J_i^c(q)^{\mathrm{T}} \lambda_i = M(q,\theta)\ddot{q} + b(q,\dot{q},\theta), \qquad 11.$$

which is further confounded by redundancy for the contact forces in many contact scenarios. Such a model encompasses the description of legged robots walking and running in contact with the ground, nonprehensile manipulation of objects, and so on. The fact that only the motion of the system is observed [e.g., $y = (q, \dot{q}) + \epsilon$] essentially results in added complexity to the problem in which robust determination of the contact states (i.e., contact points, modes, and forces) has to be addressed within the parameter identification process.

Fazeli et al. (37) explored the use of a time-stepping linear complementarity problem formulation to determine the contact states within the equation error formulation. Also, parameter identifiability was revealed under several cases with contact modes known a priori. However, due to the nature of the equation error formulation, in which perfect, noise-free state measurements are implicitly assumed, the contact timing, mode, and points must be determined directly via the raw state measurements. Incorrect specification of the contact states can bias the resulting parameter estimates, which also has a significant impact on the accuracy of any forward simulations using the identified model.

To address this issue, it would be more appropriate to expose these contact uncertainties incurred by the possible state measurement errors under the simulation error formulation, in which the state estimation problem is implicitly involved (38) (see Equation 6). Modern differentiable physics simulators provide gradients of the state evolution with respect to the model parameters, with which system identification of various (rigid and soft) robotic systems undergoing contact has been studied. These methods are most often based on the simulation error criterion and have relied primarily on shooting methods (39–45). However, reliable gradient-based optimization of state trajectories undergoing contacts is, in general, an open problem due to the inherent discontinuous nature of the contact dynamics and the associated combinatorial nature of optimization over contacts. This area remains one of active research (45–48).

4. A GEOMETRIC TAKE ON ROBOT MODEL PARAMETERS

4.1. Revisiting the Parameter-Centric View on Identification Error

To continue the discussion initiated in Section 2.1, in the context of the general model parameter identification problem, it is difficult to foresee the impact of parameter errors on model performance beyond the available limited and noisy data samples.

That being said, the physical nature of the parameters to be identified in physics-based robot models offers a higher level of interpretability and predictability in the identification process. To elaborate, mass–inertial parameters provide a quadratic representation of kinetic energy in (interconnected) rigid-body systems. Stiffness parameters define components that store elastic potential energy, while friction parameters describe the model of dissipative forces. The inherent connection of these parameters to underlying physical phenomena can guide the identification process, preventing identified models from overfitting to aberrant aspects in the data. For instance, mass–inertial parameters resulting in a negative definite mass matrix or negative values for friction or stiffness parameters would no longer accurately capture inherent physical characteristics. Similarly, in the case of a humanoid robot, center-of-mass parameters that deviate significantly from the characteristics of its physical body would not provide a sensible estimate of the risk of falling. Given these considerations, a natural question arises: Is there a systematic approach to measure the amount of information the data samples carry about the parameters in a way that accounts for their inherent physical meanings?

In this section, we show how a geometric characterization of the space of physical parameters within robot dynamic models has facilitated the recent development of robust and physically consistent identification methods. These methods have shown notable improvements in generalization performance, particularly when dealing with limited and noisy data. We begin by characterizing the space of physical parameters constituting robot dynamic models (Section 4.2). This characterization provides a bridge to show how the mass–inertial parameters of a robot reside in a curved Riemannian space (Section 4.3), which allows perturbations in the mass–inertial properties to be measured in a coordinate-invariant manner. Then, in Section 4.4, we answer the question raised above by demonstrating a systematic way to construct a set of geometric information measures, which can be used to derive a physically meaningful, invariant confidence interval for assessing practical identifiability, and also to proceed to generate optimal excitation trajectories for identification. Finally, Section 4.5 discusses geometric regularization methods within the context of both offline identification and online adaptive control.

4.2. Characterization of Physical Parameter Space

A direct approach to guaranteeing that the model produces physically consistent long-term predictions is to restrict the parameters to those realizable in the physical world. That is, we seek to define the space Θ so that every element is realizable in the physical world. For instance, mass or joint stiffness and friction coefficients should always be positive, while a spatial stiffness or damping matrix should be positive definite.

Things become a bit more involved when defining the correct necessary and sufficient condition for the mass–inertial parameters of a rigid body to be physically realizable. To illustrate, the mass–inertial parameters ϕ of a single rigid body constitute 10 parameters represented in vectorized form as

$$\phi = [m, h^{\mathrm{T}}, I^{xx}, I^{yy}, I^{zz}, I^{xy}, I^{yz}, I^{zx}]^{\mathrm{T}} \in \mathbb{R}^{10}, \qquad 12.$$

where $m \in \mathbb{R}$ is the mass; $h = m \cdot p \in \mathbb{R}^3$ is the first mass moment, with p being the position of the center of mass; and $I \in \mathbb{R}^{3\times3}$ denotes the 3×3 symmetric tensor representation of rotational

inertia. A necessary condition for physical consistency was first employed in the context of robot mass–inertial parameter identification by Li & Slotine (49) and Yoshida and colleagues (50, 51); that is, the mass should be positive, $m > 0$, and the rotational inertia at the center of mass should be positive definite, $I - [h][h]^{\mathrm{T}}/m \succ 0$, where $[\cdot]$ is a skew-symmetric representation of a three-dimensional vector (52). This condition was later formalized by Sousa & Cortesao (32) as a linear matrix inequality constraint, which allowed the nonlinear physical consistency condition to be incorporated within a convex semidefinite programming formulation for identification. Then, Traversaro et al. (33) pointed out the complete necessary and sufficient condition for physical consistency on inertial parameters, which can also be found in the rigid-body dynamics literature (53, pp. 43–44). The remaining condition for sufficiency was the triangle inequality condition on the eigenvalues of the rotational inertia tensor. More recently, Wensing et al. (34) formalized the full physical consistency condition in a linear matrix inequality as

$$P(\phi) \triangleq \begin{bmatrix} \Sigma & h \\ h^{\mathrm{T}} & m \end{bmatrix} \succ 0, \tag{13.}$$

where there exists a one-to-one linear correspondence between the above pseudoinertia matrix $P(\phi)$ and ϕ via $\Sigma = \frac{1}{2}\mathrm{tr}(I)\mathbb{I}_3 - I$ and $I = \mathrm{tr}(\Sigma)\mathbb{I}_3 - \Sigma$. Today's modern robot simulators, such as MuJoCo (54), support built-in validation for inertial parameters to satisfy this condition for improved simulation fidelity and better practice of model-based engineering.

4.3. Geometry of Physical Parameter Space

Importantly, the condition in Equation 13 precisely represents the fact that mass–inertial parameters should be strictly realizable from a nonnegative mass density function of a rigid body (34). Based on this insight, Lee & Park (55) proposed a coordinate-invariant distance metric on the mass–inertial parameters that measures perturbations to the underlying mass distribution in a physically meaningful way. Specifically, the affine-invariant Riemannian metric (56) between two mass–inertial parameter vectors ϕ_1 and ϕ_2 can be given as

$$d(\phi_1, \phi_2)^2 = \frac{1}{2}\mathrm{tr}\left(\mathrm{Log}\left((P(\phi_1)^{-1}P(\phi_2)\right)^2\right), \tag{14.}$$

where Log denotes the matrix logarithm.

As noted by Lee et al. (57), while there can be many other possible choices of distance metric that encode different useful physical meanings, coordinate invariance is firmly required since an arbitrary choice of body-fixed coordinates or units can represent the mass–inertial parameters. To explain, given a generic pseudoinertia $P \in \mathcal{P}(4)$ (i.e., the set of 4×4 positive definite matrices), any change of coordinate frame, or change in physical units or scale, transforms the pseudoinertia P to GPG^{T} for some $G \in GL(4)$, where $GL(n)$ denotes the set of $n \times n$ invertible matrices (see equations 10–13 in Reference 55). This operation represents a $GL(4)$ group action $*$ on $\mathcal{P}(4)$ defined by $G * P \triangleq GPG^{\mathrm{T}}$. A key property of the affine-invariant metric is that it is invariant under this group action (56).[4] Since coordinate/scale changes represent a subset of all such transformations GPG^{T}, this property guarantees coordinate and scale/unit invariance of the proposed metric in Equation 14. While numeric values transform according to the transformation of coordinates, the intrinsic measure of how two mass–inertial parameter vectors differ should not depend on this choice.

As discussed in the following sections, some nontrivial convex approximations to the Riemannian distance metric have proven to be useful for developing computationally tractable and

[4]That is, given matrices $P_1, P_2 \in \mathcal{P}(n)$ and any $G \in GL(n)$, the geodesic distance $d_{\mathcal{P}(n)} : \mathcal{P}(n) \times \mathcal{P}(n) \to \mathbb{R}$ corresponding to the affine-invariant Riemannian metric satisfies $d_{\mathcal{P}(n)}(P_1, P_2) = d_{\mathcal{P}(n)}(G * P_1, G * P_2)$.

efficient algorithms. The Bregman divergence (57) associated with the negative log determinant $F(\phi) = -\log(|P(\phi)|)$ provides a second-order approximation of the squared Riemannian distance, given as

$$d_{\mathrm{F}}(\phi_1 \| \phi_2)^2 = \log \frac{|P(\phi_2)|}{|P(\phi_1)|} + \mathrm{tr}\big(P(\phi_2)^{-1} P(\phi_1)\big) - 4, \tag{15.}$$

which is convex in its first argument. Also, a quadratic approximation can be given by considering a constant (differential) Riemannian metric evaluated at some given nominal value ϕ_0:

$$d_0(\phi_1, \phi_2)^2 = \frac{1}{2}\mathrm{tr}\left(\left[(P(\phi_0)^{-1} P(\phi_1 - \phi_2)\right]^2\right) \equiv (\phi_1 - \phi_2)^{\mathrm{T}} g(\phi_0)(\phi_1 - \phi_2), \tag{16.}$$

where $g(\cdot)$ is the pullback of the affine-invariant Riemannian metric on $\mathcal{P}(4)$ to $\mathbb{R}^{10}$ under the mapping $P(\cdot)$. This squared metric is also a case of a Bregman divergence but associated with the function $F(\phi) = \phi^{\mathrm{T}} g(\phi_0)\phi$. Importantly, both of these approximate distance measures admit the same coordinate invariance property as the Riemannian distance.

As previously mentioned, other physical parameters, such as stiffness, friction, and damping, can be readily identified as positive tensors. It is possible to demonstrate that the same affine-invariant Riemannian metric and its approximations provide well-defined coordinate-invariant distance measures for these parameters. Further, as noted in section 5.3 of Reference 58, the affine-invariant Riemannian manifold structure can be generalized to be imposed on an arbitrary convex set of mass–inertial parameters. This generalization can be accomplished by inducing a Riemannian metric as the Hessian of a strictly convex, twice-differentiable barrier function on the set, which then gives rise to a Hessian manifold structure. This approach can be used, for example, to impose variable bounds or other linear constraints on the parameters beyond those related to physical consistency (58).

4.4. Geometric Information Measure

If we refer to Equation SB1 (see the sidebar titled The Data Collection Problem), we can see that selecting a meaningful scalar measure $\sigma(\cdot)$ as a function of the information matrix amounts to selecting a meaningful distance metric to quantify the variability of the estimation error in the parameter space. The so-called A-optimality criterion (10) is constructed by choosing the inverse-trace operator for σ, i.e., $\mathrm{tr}(\mathcal{I}(\bar{\theta})^{-1})$. Noting that the inverse of the information matrix serves as the covariance matrix $\mathrm{var}[\hat{\theta}]$ for the efficient unbiased estimator $\hat{\theta}$, one can rewrite it as

$$\mathrm{tr}(\mathcal{I}(\bar{\theta})^{-1}) = \mathrm{tr}(\mathrm{var}[\hat{\theta}]) = \mathbb{E}_{\hat{\theta}}\left[\|\bar{\theta} - \hat{\theta}\|^2\right]. \tag{17.}$$

Clearly, the standard A-optimality criterion exhibits the standard Euclidean metric as a distance metric on parameters. This choice is a sensible one if the representation of the parameters θ exhibits a canonical coordinate choice under which all entries of the parameters are on a similar scale. However, as mentioned earlier, physical parameters like mass–inertial parameters—or, more accurately, the base parameters—exhibit arbitrary choice of coordinates and linear reparameterizations by the user. The standard Euclidean metric not only is coordinate dependent but also does not capture the multiscale nature of physical parameters that come with different units and scales.

Instead, an A-optimality criterion that is akin to the form $\mathbb{E}_{\hat{\theta}}\big[d(\bar{\theta}, \hat{\theta})^2\big]$, where $d(\cdot, \cdot)$ is some coordinate-invariant physically meaningful distance metric, is a more practically appealing choice. Lee et al. (59) reformulated various choices of existing coordinate-dependent optimality criteria, including the alphabet-optimality criteria (10) and the condition number, via definition as (cf. Equation SB1)

$$\sigma\left(\mathcal{I}(\bar{\theta}, u_{1:N}) \cdot H_0^{-1}\right), \tag{18.}$$

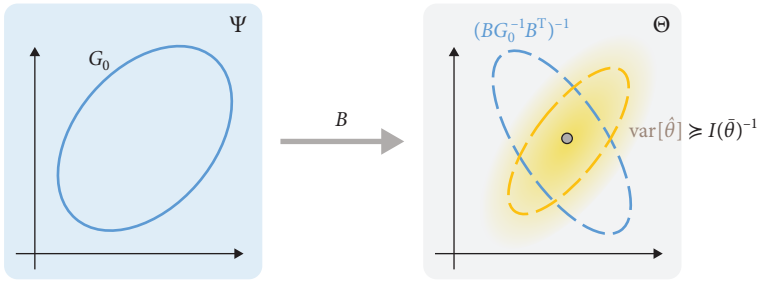

Figure 3

Example of how the parameter estimation variance or information (*yellow dashed ellipsoid*) can be quantified relative to the metric $H_0 = (BG_0^{-1}B^T)^{-1}$ (*blue dashed ellipsoid*) inherited from the metric G_0 originally defined on the standard parameter space Ψ.

where $\sigma(X)$ denotes a symmetric function of the eigenvalues of matrix X, and the constant normalization matrix $H_0 = (BG_0^{-1}B^T)^{-1}$ can be understood as the projection of the constant pullback metric G_0 [analogous to $g(\phi_0)$ in Equation 16] defined over the standard parameters $\psi = [\phi_1, \ldots, \phi_n] \in \Psi$ to the reduced structurally identifiable parameter space under the particular base parameter representation B, i.e., $\theta = B\psi \in \Theta$. As shown in **Figure 3**, this can also be viewed as the coordinate-invariant measure of how much the distribution of the parameter estimates is distorted relative to the natural choice of metric predefined over the parameter space Θ. In effect, this geometric framework allows for a formal, systematic way in which to normalize the information matrix so that the ensuing optimal excitation trajectory generation problem leads to the consideration of lighter links needing to be more excited than the heavier ones, as mass–inertial parameter values are more likely to be negative definite under the same scale of estimation variance.

As noted by Lee et al. (59), the inverse of the eigenvalues[5] of the normalized information matrix can also be used to assess the practical identifiability of the parameters based on a single scale-free threshold value. Meanwhile, numerical studies provided by Lee et al. (59) have also shown that the fraction of practically identifiable parameters, among the structurally identifiable ones, is considerably restricted in practice, especially for high-dimensional systems such as humanoid robots. This finding highlights the need for a regularized formulation of the parameter identification problem to effectively mitigate such a practical identifiability issue within purely data-driven parameter estimation by incorporating prior information.

4.5. Geometric Regularization Techniques

One unique aspect of physics-based models, in comparison with generic function approximation models, is that obtaining reasonably accurate and physically plausible nominal parameters is viable prior to collecting data. This can be achieved through various means, such as utilizing CAD data or making a rough guess. In light of the practical challenges due to factors such as data sufficiency, noise, and structural errors, it is crucial for practitioners to recognize that full precise identification of robot models is often impractical and that the nominal model of a robot, in addition to input–output data samples, is a valuable and viable source of information that can be leveraged in identification. More concretely, many of these difficulties can be mitigated by appealing to appropriate regularization of the parameter identification objective using the nominal parameters.

[5]The eigenvalues provide a scale-free measure of parameter estimation variance projected along the corresponding eigenvectors under the metric $(BG_0^{-1}B^T)^{-1}$.

GEOMETRIC REGULARIZATION IN ADAPTIVE CONTROL

Bregman divergence measures (e.g., Equation 15 or 16) for geometric regularization in identification have also played a key role in the design of recent geometric adaptive control laws (61, 62). In that context, one can show stability of the adaptive laws using a Lyapunov function that includes the terms $D(\overline{\psi} \,\|\, \hat{\psi}) := \sum_i d_F(\overline{\phi}_i \,\|\, \hat{\phi}_i)^2$, where $\hat{\psi}$ represents the parameter estimate. Remarkably, the asymptotic solution of the adaptation laws developed therein implicitly regularizes the solution, in that persistently exciting trajectory references lead to $\lim_{t\to\infty} \hat{\psi}(t) = \operatorname{argmin}_{\psi \in \overline{\psi}+\mathcal{N}} D(\psi \,\|\, \hat{\psi}(0))$ (61). More generally, in the absence of persistently exciting references, the parameters converge to a minimizer within a (higher-dimensional) affine subspace that contains $\overline{\psi} + \mathcal{N}$ (for details, see 61).

To explain, assuming that some prior distribution on the standard parameters $\psi = [\phi_1, \ldots, \phi_{N_L}]$ is given as $p(\psi)$, the maximum a posteriori formulation (60) aims to optimize the posterior distribution over ψ as $\min_\psi -\log p(\psi|\mathcal{D}) \propto L(B\psi) - \log p(\psi)$, where the previous MLE objective $L(\theta) = L(B\psi)$ (Equation 3) defined over the base parameters is now regularized with the negative logarithm of the prior model over ψ. Consequently, the regularization term is chosen to be proportional to some distance measure to the nominal parameters ψ_0—i.e., the maximum a posteriori optimization takes the form

$$\min_{\psi} L(B\psi) + \gamma d(\psi, \psi_0)^2. \tag{19.}$$

The base parameter estimate can be simply recovered by $\hat{\theta} = B\hat{\psi}$, where $\hat{\psi}$ is given as the solution of the regularized identification objective above.

Here, the choice of distance metric d greatly impacts the generalization performance, which essentially dictates a scalar measure of how the multivariate parameter estimates from data samples would deviate from the nominal parameters. The use of the geometric distance metric in Equation 14 or its convex approximations in Equation 15 or 16 is significantly more generalizable than, e.g., the standard Euclidean metric, as they capture the perturbations in the mass–inertial parameters in a coordinate-invariant and physically meaningful way (see figure 2 of Reference 57). Recent theoretical breakthroughs regarding implicit regularization (61) have likewise translated these benefits to adaptive control settings (see the sidebar titled Geometric Regularization in Adaptive Control). Overall, geometric regularization methods have shown practical significance for robustness and generalization performance in various systems and scenarios, including online parameter identification of robot manipulators with proprioceptive actuation, generalization of fixed-base dynamics identification results for quadruped robot legs to the full floating-base dynamics model, and reduced base-link dynamics identification for a humanoid model under significant levels of measurement noise.

5. REDUCING STRUCTURAL BIAS IN ROBOT MODELS

While previous sections focused on system identification methods that exploit physical meanings of parameters constituting a classical parameterization of robot dynamics models, this section explores various extended classes of parameterized models that aim to alleviate the structural errors (introduced in Section 2.3.1) in a physically meaningful way.

5.1. Kinodynamic Model Identification

Existing methods for robot identification generally separate kinematic identification from dynamic identification; the kinematic parameters are either identified first or assumed to be provided

by manufacturers (e.g., via CAD), followed by the identification of mass–inertial parameters. This separation is largely for reasons of convenience; given that the dynamic model is nonlinear with respect to the kinematic parameters, the linearity-in-parameter property fundamental to many existing robot model identification methods holds only if the kinematic parameters are fixed.

These sequential approaches, however, could potentially introduce bias due to errors in kinematic parameters. Specifically, as reported by Kwon et al. (9), poorly identified kinematic parameters can lead to an uncorrectable bias in the dynamic model, resulting in errors in the mass–inertial parameters that are many times greater than the kinematic parameter errors. To address this, the authors proposed a unified identification framework that jointly identifies the kinematic and dynamic model parameters by minimizing the sum of both errors as

$$\min_{\theta_{\text{dyn}},\theta_{\text{kin}}} \quad L_{\text{dyn}}(\theta_{\text{dyn}},\theta_{\text{kin}}) + \alpha \cdot L_{\text{kin}}(\theta_{\text{kin}}), \qquad 20.$$

where θ_{dyn} and θ_{kin} denote the dynamic and kinematic parameters (e.g., joint screws), respectively, and L_{dyn} and L_{kin} denote the dynamic and kinematic identification objective functions, respectively. The kinematic identification objective, for example, is an error between the end-effector poses measured by cameras and the kinematic model estimates.

Formally, this approach can be derived by expanding the observation y in Equation 2 to include the kinematic measurement [e.g., $y = (x, T) = (x, \text{FK}_{\theta_{\text{kin}}}(x) + \epsilon)$, where T is the end-effector pose measurement and $\text{FK}_{\theta_{\text{kin}}}$ denotes the forward kinematics mapping] and applying the MLE argument (i.e., Equation 3). Allowing for the update of kinematic parameters to also reduce the dynamic error can mitigate the structural error induced by the kinematic parameter error. Importantly, under the MLE argument, the weight α can be determined to represent the relative accuracy of kinematic and dynamic sensors (e.g., camera and joint torque sensor) as $\alpha = \sigma_{\text{dyn}}/\sigma_{\text{kin}}$, where σ_{dyn} and σ_{kin} denote the sensor noise scales. This relationship implies that when the kinematic sensor is highly inaccurate, α becomes zero (i.e., $\sigma_{\text{kin}} \gg 1$), rendering the kinematic error less critical in identifying the kinematic parameters. Conversely, if the kinematic sensor is noise free (for example, with a high-performance motion capture system), α approaches infinity, making the process similar to the traditional decoupled identification. This unified method is especially advantageous when precise kinematic parameters or sensors are unavailable, and substantial model bias is otherwise introduced.

Alternatively, by substituting the error criterion with the simulation error (as in Equation 6), Kolev & Todorov (38) explored kinodynamic model identification for contact manipulation. In this study, the dynamic parameters included contact model parameters (such as stiffness and damping), with both state trajectories and model parameters estimated concurrently.

Note that while the kinodynamic model identification has extended the candidate model set to deal with the structural error, it still consists only of physically interpretable parameters and strictly adheres to first principles (i.e., the dynamics of articulated rigid-body systems). In the subsequent sections, we explore more data-driven methods designed to compensate for residual errors that the existing laws of physics cannot fully address.

5.2. Discrepancy Modeling Approaches

Data-driven modeling approaches that partly augment existing physics-based models have proven more generalizable and data efficient than relying on neural networks or other generic function approximators to model the complete robot kinematics and dynamics. Some of these methods directly append deterministic data-driven models to the forward or inverse dynamics equations. These methods are designed to model residual forces acting on the bodies or joints that are

difficult to model analytically, such as nonlinear state-dependent frictions or aerodynamic drag forces, or to capture non-Markovian phenomena such as hysteresis, backlash, or unmodeled elasticity with memory-based models (for examples of such methods, see, e.g., References 7 and 63–65). In addition, Hwangbo et al. (8) proposed a technique to learn a nonlinear recurrent neural network mapping from low-level actuator commands to more conventional inputs (e.g., joint torques) accepted by existing physics-based simulators. This approach has been shown to be effective for modeling complex input–output dynamics of actuators subject to nonlinear elasticity, such as series-elastic actuators. Stochastic models based on deep generative models (66) or nonparametric models such as Gaussian processes (67) have also been used to model the uncertainty in the residual error.

Although discrepancy modeling approaches significantly reduce the extent to which data-driven models need to learn from data compared with pure data-driven models, they do not necessarily ensure the preservation of many system characteristics inherent to the original physics-based model. Therefore, it is essential to carefully validate the model on a wide distribution of test samples to ensure its reliability and accuracy. In addition, the deliberate incorporation of inductive biases in the augmented data-driven model can also be a practical and viable solution. In the next section, we highlight some notable approaches in this direction for modeling contact dynamics, which build upon the classic contact mechanics in a way that explicitly ensures the nonpenetration of colliding bodies.

5.3. Putting Physics in Data-Driven Model Learning

Up to this point, we have identified physics-based models as those that characterize the input–output behavior of physical systems using fundamental principles or laws of physics. These models explicitly represent physical parameters, such as mass–inertia, joint screws, and stiffness, which are all tangible and measurable. On the other hand, data-driven modeling approaches (67) typically refer to bottom-up methods of deducing new laws from experimental observations, with the caveat that the parameters within these models do not necessarily possess an explicit physical meaning. However, this observation does not mean that data-driven models must be arbitrarily complex in order to learn everything from data. Recent works have shown that a new class of models can be constructed to deliberately exhibit some essential characteristics of physical systems via so-called inductive biases.

Below, we classify a range of beneficial inductive biases pertinent to the modeling of robotic systems. While the majority of these attributes are currently satisfied and incorporated within established physics-based models, the overarching technical objective is to reconstruct these inductive biases with enhanced flexibility, thereby facilitating the modeling of an expanded repertoire of complex physical systems.

5.3.1. Energy conservation. Embracing the concept of energy has played a pivotal role in the implementation of model-based engineering approaches within traditional mechanics-based robot models, such as those employing Lagrangian mechanics to characterize coupled rigid bodies. Key elements of these methodologies include developing stable integrators (68–70) and energy-based controllers (71, 72). Recent advancements in data-driven modeling techniques have shown ways to construct a new class of deep neural networks that explicitly inherit essential properties, such as energy conservation and passivity, of Hamiltonian and Lagrangian mechanics by constructing a valid kinetic energy function of the system (73), i.e., $E = \frac{1}{2}\dot{q}^{\mathrm{T}} M_\theta(q)\dot{q} > 0$. These models straightforwardly demonstrate that the aforementioned energy-based methodologies can be applied in a manner comparable to their traditional counterparts (74). More recently, these models have been extended to be augmented with classical contact dynamics to model legged

robots and robotic manipulators involving contacts and collisions, which introduce discontinuities in the states (75).

5.3.2. Energy dissipation. Robotic systems consist of several components that contribute to the dissipation of energy in complex ways. One of the primary factors that leads to energy dissipation is friction, which can be highly nonlinear and state dependent. Despite its complexity, the presence of friction is useful for control applications, mainly due to its dissipative nature. Specifically, the energy $\mathcal{E}$ of an uncontrolled system with generalized coordinates q should dissipate over time, i.e., $\dot{E} = \dot{q}^{\mathrm{T}} f(q, \dot{q}) \leq 0$, where $f(q, \dot{q})$ represents the generalized forces of friction. A data-driven configuration-dependent friction model has proven effective for modeling complex tendon-driven robots, in which the coupling of joints forming closed kinematic chains can cause nonlinear variations of friction coefficients (7). For dynamic friction effects subject to, for instance, hysteresis or stick–slip motions, a more general condition can be derived from the strict passivity condition, i.e., $\dot{q}^{\mathrm{T}} f(z, q, \dot{q}) \geq \dot{W}(z(t))$ for all t, where W is a positive storage function of the internal state z. While energy-dissipative models for dynamic friction have been studied primarily in one-dimensional systems (76), it is potentially viable to explore a more general class of multidimensional dynamic friction models that satisfy strict passivity.

5.3.3. Contact. Several studies have shown that standard rigid-contact solvers used in state-of-the-art rigid-body dynamics simulators fail to precisely capture the contact behavior in the real world (48). While there have been many data-driven modeling approaches to directly learn the contact dynamics from data, these approaches often fail to guarantee the most salient properties of contact interactions, which are nonpenetration of bodies and energy dissipation subject to contact friction.

One of the major issues in simulating contact behaviors lies in the robust and accurate determination of contact points/normals and modes. Also, some of the ad hoc heuristics adopted in off-the-shelf rigid-body simulators are driven partly by real-time computational constraints rather than fully prioritizing simulation accuracy (77). Recently, data-driven models have augmented the classical contact solvers in a nontrivial way to preserve the nonpenetrating and dissipative behavior of contact while being flexible enough to match reality. These methods include data-driven learning of robust contact mode switch detection (78) as well as contact clustering (77). In addition, data-driven learning for the smooth representation of shapes has been studied within the identification of contact dynamics to alleviate shape uncertainty and contact-induced discontinuities. These data-driven shape representations include interbody signed distance functions (79) and neural density fields (80), which can be straightforwardly adopted in standard differentiable physics engines.

5.3.4. Topology and graphs. It is evident that robots with articulated bodies possess an inherent graphical structure due to their physical connectivity. Additionally, the contact interactions between robots and their surrounding environments also exhibit a graphical structure dictated by the intermittent kinematic structure of contact (81). Recently, graph neural network models have gained popularity because they explicitly aim to capture and leverage this relational inductive bias. These models impose this structure by appropriately assigning state variables to each node in the graph and constraining computations to propagate through prespecified (or potentially learnable) edge connections. However, these methods are currently limited to simulation experiments (82) and scenarios involving simple particle–object interactions (83, 84). We believe that one of the significant advantages that comes with the way graphical structure is embedded in classical mechanics-based models lies in their compositionality. For example, if one has a completely separate pair of models for a robot and an object, it becomes possible to evaluate their interactions

in a zero-shot manner. In that regard, whether these graphically structured data-driven models can effectively demonstrate generalization performance within arbitrary compositions of graphs remains an open problem.

5.3.5. Invariance and symmetry. It is important to note that while the choice of coordinate frames to describe the physical output variables (such as end-effector poses) or parameters (such as mass–inertia and shapes) is entirely up to the user, the results are completely invariant—or, more precisely, equivariant[6]—to these choices. This property essentially makes the universal adoption of standard robot description formats, such as URDF, MJCF, and SDF, with arbitrary coordinate choices viable. Indeed, the result of any physical phenomenon must not be affected by the particular choices of coordinate one adopts to describe them numerically. While this may sound somewhat obvious, such a property is not easily attainable in many data-driven models that do not exhibit invariance or equivariance properties subject to certain group transformations on the input–output variables and/or parameters. Recent group-equivariant networks are beginning to be adapted to various dynamics learning problems in robotics and have shown superior generalization performance and sample efficiency with respect to the variations in shapes and poses. The current applications range from grasp quality prediction (85) to tabletop object pushing and the learning of interaction dynamics (86, 87) to dynamic modeling of multilegged robots (88).

6. CONCLUSION

Constructing accurate and reliable descriptions of robotic systems interacting in the real world is naturally posed as a data-driven learning problem from input–output data samples. Starting from the generic black-box system identification view of the dynamic model identification and learning problem, this review has pointed out various practical concerns across stages of the system identification process. As applied to robotics, we have focused primarily on addressing the availability of a sufficient amount of data and the generalizability of the modeling and identification methods.

Robotics continues to deal with problems related to interactions that occur in the physical world. Undoubtedly, physics represents the most powerful domain knowledge and useful inductive bias inherent in this setting. In light of this view, we have shown how explicit considerations of physics-based knowledge in statistical data-driven approaches to system identification have enabled many recent advances for enhanced robustness and generalizability in the face of limited and noisy data.

It is important to recognize that system identification should not be considered an ultimate goal in and of itself; rather, it is a valuable tool for a wide range of targeted robotics applications. In line with this understanding, the controls and reinforcement learning community is increasingly committed to developing system identification methods that are directly aligned with control and task objectives (26, 89, 90). While this review did not extensively explore these ideas, they represent exciting prospects for the field's future. Through these and other advancements, we hold hope that ongoing developments will facilitate the promotion of robust, sample-efficient, and generalizable robot models that are well equipped to support the complex tasks robots are expected to perform. As these systems interact with and navigate the physical world, we have a growing opportunity to leverage the vast structural richness it provides.

[6]A mapping $f : \mathcal{X} \to \mathcal{Y}$ is equivariant under the transformation group $\mathcal{G}$ if it satisfies the relation $\mathcal{S}_g \circ y = f(\mathcal{T}_g \circ x)$ for all $x \in \mathcal{X}$, $y \in \mathcal{Y}$, and $g \in \mathcal{G}$, where $\mathcal{T}_g : \mathcal{X} \to \mathcal{X}$ and $\mathcal{S}_g : \mathcal{Y} \to \mathcal{Y}$ are the group actions of g on $\mathcal{X}$ and $\mathcal{Y}$, respectively. Normally, these group actions are given as the coordinate transformation rules on the respective spaces. If $\mathcal{S}_g$ is an identity mapping, then f is an invariant mapping.

SUMMARY POINTS

1. A recent geometric perspective on the mass–inertial parameters of rigid robot dynamics model has facilitated the development of robust and physically consistent identification methods that have led to notable improvements in model generalization, particularly when dealing with limited and noisy data.
2. We identified and corrected some long-standing issues with the established practice of first performing kinematic identification, followed by mass–inertial parameter identification. Specifically, poorly identified kinematic parameters can lead to an uncorrectable bias in the dynamic model, resulting in errors in the dynamic parameters that are many times greater than the kinematic parameter errors. A unified kinodynamic identification method was described that leads to more accurate identification of both the kinematic and dynamic parameters.
3. We described ways in which robot models can be augmented with data-driven models or entirely reconstructed in a way that respects some of the important physics-based inductive biases with enhanced flexibility, thereby facilitating the modeling of an expanded repertoire of complex physical systems.

DISCLOSURE STATEMENT

The authors are not aware of any affiliations, memberships, funding, or financial holdings that might be perceived as affecting the objectivity of this review.

ACKNOWLEDGMENTS

F.C.P. was supported in part by National Research Foundation of Korea (NRF)–Ministry of Science and Information and Communication Technologies (MSIT) grant RS-2023-00208052, Institute for Information Communication Technology Planning (IITP)–MSIT grant 2021-0-02068 [Seoul National University (SNU) AI Innovation Hub], IITP-MSIT grant 2022-0-00480 (Training and Inference Methods for Goal-Oriented AI Agents), the SNU Artificial Intelligence Institute, the SNU Institute of Advanced Machinery and Design, the SNU BK21+ Program in Mechanical Engineering, and the SNU Institute for Engineering Research. P.M.W. was supported in part by National Science Foundation award CMMI-2220924 with a sub-award to the University of Notre Dame.

LITERATURE CITED

1. Kristensen NR, Madsen H, Jørgensen SB. 2004. Parameter estimation in stochastic grey-box models. *Automatica* 40(2):225–37
2. Schoukens J, Ljung L. 2019. Nonlinear system identification: a user-oriented road map. *IEEE Control Syst. Mag.* 39(6):28–99
3. Wu P, Escontrela A, Hafner D, Abbeel P, Goldberg K. 2023. DayDreamer: world models for physical robot learning. In *Proceedings of the 6th Conference on Robot Learning*, ed. K Liu, D Kulic, J Ichnowski, pp. 2226–40. Proc. Mach. Learn. Res. 205. N.p.: PMLR
4. Brunot M, Janot A, Carrillo F, Cheong J, Noël JP. 2020. Output error methods for robot identification. *J. Dyn. Syst. Meas. Control* 142(3):031002
5. Swevers J, Ganseman C, Tukel DB, De Schutter J, Van Brussel H. 1997. Optimal robot excitation and identification. *IEEE Trans. Robot. Autom.* 13(5):730–40

6. Gautier M, Janot A, Vandanjon PO. 2012. A new closed-loop output error method for parameter identification of robot dynamics. *IEEE Trans. Control Syst. Technol.* 21(2):428–44
7. Choi K, Kwon J, Lee T, Park C, Pyo J, et al. 2020. A hybrid dynamic model for the ambidex tendon-driven manipulator. *Mechatronics* 69:102398
8. Hwangbo J, Lee J, Dosovitskiy A, Bellicoso D, Tsounis V, et al. 2019. Learning agile and dynamic motor skills for legged robots. *Sci. Robot.* 4(26):eaau5872
9. Kwon J, Choi K, Park FC. 2021. Kinodynamic model identification: a unified geometric approach. *IEEE Trans. Robot.* 37(4):1100–14
10. Pukelsheim F. 2006. *Optimal Design of Experiments*. Philadelphia: Soc. Ind. Appl. Math.
11. Pronzato L. 2008. Optimal experimental design and some related control problems. *Automatica* 44(2):303–25
12. Bonnet V, Fraisse P, Crosnier A, Gautier M, González A, Venture G. 2016. Optimal exciting dance for identifying inertial parameters of an anthropomorphic structure. *IEEE Trans. Robot.* 32(4):823–36
13. Brunke L, Greeff M, Hall AW, Yuan Z, Zhou S, et al. 2022. Safe learning in robotics: from learning-based control to safe reinforcement learning. *Annu. Rev. Control Robot. Auton. Syst.* 5:411–44
14. Yasa O, Toshimitsu Y, Michelis MY, Jones LS, Filippi M, et al. 2023. An overview of soft robotics. *Annu. Rev. Control Robot. Auton. Syst.* 6:1–29
15. Atkeson CG, An CH, Hollerbach JM. 1986. Estimation of inertial parameters of manipulator loads and links. *Int. J. Robot. Res.* 5(3):101–19
16. Wensing PM, Niemeyer G, Slotine JJE. 2023. A geometric characterization of observability in inertial parameter identification. arXiv:1711.03896 [cs.RO]
17. Mayeda H, Yoshida K, Osuka K. 1988. Base parameters of manipulator dynamic models. In *1988 IEEE International Conference on Robotics and Automation*, Vol. 3, pp. 1367–72. Piscataway, NJ: IEEE
18. Gautier M, Khalil W. 1988. A direct determination of minimum inertial parameters of robots. In *1988 IEEE International Conference on Robotics and Automation*, Vol. 3, pp. 1682–87. Piscataway, NJ: IEEE
19. Khalil W, Kleinfinger JF. 1987. Minimum operations and minimum parameters of the dynamic models of tree structure robots. *IEEE J. Robot. Autom.* 3(6):517–26
20. Ros J, Iriarte X, Mata V. 2012. 3D inertia transfer concept and symbolic determination of the base inertial parameters. *Mech. Mach. Theory* 49:284–97
21. Gautier M. 1991. Numerical calculation of the base inertial parameters of robots. *J. Robot. Syst.* 8(4):485–506
22. Van Huffel S, Vandewalle J. 1991. *The Total Least Squares Problem: Computational Aspects and Analysis*. Philadelphia: Soc. Ind. Appl. Math.
23. Janot A, Vandanjon PO, Gautier M. 2013. A generic instrumental variable approach for industrial robot identification. *IEEE Trans. Control Syst. Technol.* 22(1):132–45
24. Janot A, Vandanjon PO, Gautier M. 2009. Using robust regressions and residual analysis to verify the reliability of LS estimation: application in robotics. In *2009 IEEE/RSJ International Conference on Intelligent Robots and Systems*, pp. 1962–67. Piscataway, NJ: IEEE
25. Ramdani N, Poignet P. 2005. Robust dynamic experimental identification of robots with set membership uncertainty. *IEEE/ASME Trans. Mechatron.* 10(2):253–56
26. Gevers M. 2005. Identification for control: from the early achievements to the revival of experiment design. *Eur. J. Control* 11(4–5):335–52
27. Leboutet Q, Roux J, Janot A, Guadarrama-Olvera JR, Cheng G. 2021. Inertial parameter identification in robotics: a survey. *Appl. Sci.* 11(9):4303
28. Ayusawa K, Venture G, Nakamura Y. 2014. Identifiability and identification of inertial parameters using the underactuated base-link dynamics for legged multibody systems. *Int. J. Robot. Res.* 33(3):446–68
29. Venture G, Ayusawa K, Nakamura Y. 2008. Motion capture based identification of the human body inertial parameters. In *2008 30th Annual International Conference of the IEEE Engineering in Medicine and Biology Society*, pp. 4575–78. Piscataway, NJ: IEEE
30. Ogawa Y, Venture G, Ott C. 2014. Dynamic parameters identification of a humanoid robot using joint torque sensors and/or contact forces. In *2014 IEEE-RAS International Conference on Humanoid Robots*, pp. 457–62. Piscataway, NJ: IEEE

31. Del Prete A, Mansard N. 2016. Robustness to joint-torque-tracking errors in task-space inverse dynamics. *IEEE Trans. Robot.* 32(5):1091–105
32. Sousa CD, Cortesao R. 2014. Physical feasibility of robot base inertial parameter identification: a linear matrix inequality approach. *Int. J. Robot. Res.* 33(6):931–44
33. Traversaro S, Brossette S, Escande A, Nori F. 2016. Identification of fully physical consistent inertial parameters using optimization on manifolds. In *2016 IEEE/RSJ International Conference on Intelligent Robots and Systems (IROS)*, pp. 5446–51. Piscataway, NJ: IEEE
34. Wensing PM, Kim S, Slotine JJE. 2017. Linear matrix inequalities for physically consistent inertial parameter identification: a statistical perspective on the mass distribution. *IEEE Robot. Autom. Lett.* 3(1):60–67
35. Jovic J, Escande A, Ayusawa K, Yoshida E, Kheddar A, Venture G. 2016. Humanoid and human inertia parameter identification using hierarchical optimization. *IEEE Trans. Robot.* 32(3):726–35
36. Ayusawa K, Venture G, Nakamura Y. 2011. Real-time implementation of physically consistent identification of human body segments. In *2011 IEEE International Conference on Robotics and Automation*, pp. 6282–87. Piscataway, NJ: IEEE
37. Fazeli N, Kolbert R, Tedrake R, Rodriguez A. 2017. Parameter and contact force estimation of planar rigid-bodies undergoing frictional contact. *Int. J. Robot. Res.* 36(13–14):1437–54
38. Kolev S, Todorov E. 2015. Physically consistent state estimation and system identification for contacts. In *2015 IEEE-RAS 15th International Conference on Humanoid Robots*, pp. 1036–43. Piscataway, NJ: IEEE
39. Jatavallabhula KM, Macklin M, Golemo F, Voleti V, Petrini L, et al. 2021. gradSim: differentiable simulation for system identification and visuomotor control. In *The Ninth International Conference on Learning Representations*. La Jolla, CA: Int. Conf. Learn. Represent. **https://iclr.cc/virtual/2021/poster/3082**
40. Hu Y, Anderson L, Li TM, Sun Q, Carr N, et al. 2020. DiffTaichi: differentiable programming for physical simulation. In *The Eighth International Conference on Learning Representations*. La Jolla, CA: Int. Conf. Learn. Represent. **https://iclr.cc/virtual_2020/poster_B1eB5xSFvr.html**
41. Xu J, Chen T, Zlokapa L, Foshey M, Matusik W, et al. 2021. An end-to-end differentiable framework for contact-aware robot design. In *Robotics: Science and Systems XVII*, ed. D Shell, M Toussaint, MA Hsieh, pap. 8. N.p.: Robot. Sci. Syst. Found.
42. Degrave J, Hermans M, Dambre J, Wyffels F. 2019. A differentiable physics engine for deep learning in robotics. *Front. Neurorobot.* 13:6
43. Hahn D, Banzet P, Bern JM, Coros S. 2019. Real2Sim: visco-elastic parameter estimation from dynamic motion. *ACM Trans. Graph.* 38(6):236
44. Geilinger M, Hahn D, Zehnder J, Bächer M, Thomaszewski B, Coros S. 2020. ADD: analytically differentiable dynamics for multi-body systems with frictional contact. *ACM Trans. Graph.* 39(6):190
45. Werling K, Omens D, Lee J, Exarchos I, Liu CK. 2021. Fast and feature-complete differentiable physics engine for articulated rigid bodies with contact constraints. In *Robotics: Science and Systems XVII*, ed. DA Shell, M Toussaint, MA Hsieh, pap. 34. N.p.: Robot. Sci. Syst. Found.
46. Suh HJ, Simchowitz M, Zhang K, Tedrake R. 2022. Do differentiable simulators give better policy gradients? In *Proceedings of the 39th International Conference on Machine Learning*, ed. K Chaudhuri, S Jegelka, L Song, C Szepesvari, G Niu, S Sabatopp, pp. 20668–96. Proc. Mach. Learn. Res. 162. N.p.: PMLR
47. Antonova R, Yang J, Jatavallabhula KM, Bohg J. 2023. Rethinking optimization with differentiable simulation from a global perspective. In *Proceedings of the 6th Conference on Robot Learning*, ed. K Liu, D Kulic, J Ichnowski, pp. 276–86. Proc. Mach. Learn. Res. 205. N.p.: PMLR
48. Lidec QL, Jallet W, Montaut L, Laptev I, Schmid C, Carpentier J. 2023. Contact models in robotics: a comparative analysis. arXiv:2304.06372 [cs.RO]
49. Li W, Slotine JJE. 1989. An indirect adaptive robot controller. *Syst. Control Lett.* 12(3):259–66
50. Yoshida K, Osuka K, Mayeda H, Ono T. 1996. When is the set of base-parameter values physically impossible? *J. Robot. Soc. Jpn.* 14(1):122–30
51. Yoshida K, Khalil W. 2000. Verification of the positive definiteness of the inertial matrix of manipulators using base inertial parameters. *Int. J. Robot. Res.* 19(5):498–510
52. Lynch KM, Park FC. 2017. *Modern Robotics*. Cambridge, UK: Cambridge Univ. Press
53. Wittenburg J. 2008. *Dynamics of Multibody Systems*. Berlin: Springer. 2nd ed.

54. Todorov E, Erez T, Tassa Y. 2012. MuJoCo: a physics engine for model-based control. In *2012 IEEE/RSJ international conference on intelligent robots and systems*, pp. 5026–33. Piscataway, NJ: IEEE
55. Lee T, Park FC. 2018. A geometric algorithm for robust multibody inertial parameter identification. *IEEE Robot. Autom. Lett.* 3(3):2455–62
56. Moakher M. 2005. A differential geometric approach to the geometric mean of symmetric positive-definite matrices. *SIAM J. Matrix Anal. Appl.* 26(3):735–47
57. Lee T, Wensing PM, Park FC. 2019. Geometric robot dynamic identification: a convex programming approach. *IEEE Trans. Robot.* 36(2):348–65
58. Lee T. 2019. *Geometric methods for dynamic model-based identification and control of multibody systems*. PhD Thesis, Seoul Natl. Univ., Seoul, South Korea
59. Lee T, Lee BD, Park FC. 2021. Optimal excitation trajectories for mechanical systems identification. *Automatica* 131:109773
60. Presse C, Gautier M. 1992. Bayesian estimation of inertial parameters of robots. In *1992 IEEE International Conference on Robotics and Automation*, Vol. 1, pp. 364–65. Piscataway, NJ: IEEE
61. Boffi NM, Slotine JJE. 2021. Implicit regularization and momentum algorithms in nonlinearly parameterized adaptive control and prediction. *Neural Comput.* 33(3):590–673
62. Lee T, Kwon J, Park FC. 2018. A natural adaptive control law for robot manipulators. In *2018 IEEE/RSJ International Conference on Intelligent Robots and Systems (IROS)*. Piscataway, NJ: IEEE. **http://doi.org/10.1109/IROS.2018.8593727**
63. Zeng A, Song S, Lee J, Rodriguez A, Funkhouser T. 2020. TossingBot: learning to throw arbitrary objects with residual physics. *IEEE Trans. Robot.* 36(4):1307–19
64. Golemo F, Taiga AA, Courville A, Oudeyer PY. 2018. Sim-to-real transfer with neural-augmented robot simulation. In *Proceedings of the 2nd Conference on Robot Learning*, ed. A Billard, A Dragan, J Peters, J Morimoto, pp. 734–43. Proc. Mach. Learn. Res. 87. N.p.: PMLR
65. Heiden E, Millard D, Coumans E, Sheng Y, Sukhatme GS. 2021. NeuralSim: augmenting differentiable simulators with neural networks. In *2021 IEEE International Conference on Robotics and Automation*, pp. 9474–81. Piscataway, NJ: IEEE
66. Ajay A, Wu J, Fazeli N, Bauza M, Kaelbling LP, et al. 2018. Augmenting physical simulators with stochastic neural networks: case study of planar pushing and bouncing. In *2018 IEEE/RSJ International Conference on Intelligent Robots and Systems (IROS)*, pp. 3066–73. Piscataway, NJ: IEEE
67. Nguyen-Tuong D, Peters J. 2011. Model learning for robot control: a survey. *Cogn. Process.* 12:319–40
68. Marsden JE, West M. 2001. Discrete mechanics and variational integrators. *Acta Numer.* 10:357–514
69. Lee J, Liu CK, Park FC, Srinivasa SS. 2020. A linear-time variational integrator for multibody systems. In *Algorithmic Foundations of Robotics XII*, ed. K Goldberg, P Abbeel, K Bekris, L Miller, pp. 352–67. Cham, Switz.: Springer
70. Kim M, Lee Y, Lee Y, Lee D. 2017. Haptic rendering and interactive simulation using passive midpoint integration. *Int. J. Robot. Res.* 36(12):1341–62
71. Spong MW. 1996. Energy based control of a class of underactuated mechanical systems. *IFAC Proc.* Vol. 29(1):2828–32
72. Spong MW. 2022. An historical perspective on the control of robotic manipulators. *Annu. Rev. Control Robot. Auton. Syst.* 5:1–31
73. Lutter M, Ritter C, Peters J. 2019. Deep Lagrangian networks: using physics as model prior for deep learning. In *The Seventh International Conference on Learning Representations*. La Jolla, CA: Int. Conf. Learn. Represent. **https://openreview.net/forum?id=BklHpjCqKm**
74. Lutter M, Listmann K, Peters J. 2019. Deep Lagrangian networks for end-to-end learning of energy-based control for under-actuated systems. In *2019 IEEE/RSJ International Conference on Intelligent Robots and Systems (IROS)*, pp. 7718–25. Piscataway, NJ: IEEE
75. Zhong YD, Dey B, Chakraborty A. 2021. Extending Lagrangian and Hamiltonian neural networks with differentiable contact models. In *Advances in Neural Information Processing Systems 34*, ed. M Ranzato, A Beygelzimer, Y Dauphin, PS Liang, J Wortman Vaughan, pp. 21910–22. Red Hook, NY: Curran
76. Johanastrom K, Canudas-De-Wit C. 2008. Revisiting the LuGre friction model. *IEEE Control Syst. Mag.* 28(6):101–14

77. Yoon J, Lee M, Son D, Lee D. 2022. Fast and accurate data-driven simulation framework for contact-intensive tight-tolerance robotic assembly tasks. arXiv:2202.13098 [cs.RO]
78. Jiang Y, Sun J, Liu CK. 2022. Data-augmented contact model for rigid body simulation. In *Proceedings of the 4th Annual Learning for Dynamics and Control Conference*, ed. R Firoozi, N Mehr, E Yel, R Antonova, J Bohg, et al., pp. 378–90. Proc. Mach. Learn. Res. 168. N.p.: PMLR
79. Pfrommer S, Halm M, Posa M. 2021. ContactNets: learning discontinuous contact dynamics with smooth, implicit representations. In *Proceedings of the 2020 Conference on Robot Learning*, ed. J Kober, F Ramos, C Tomlin, pp. 2279–91. Proc. Mach. Learn. Res. 155. N.p.: PMLR
80. Le Cleac'h S, Yu HX, Guo M, Howell T, Gao R, et al. 2023. Differentiable physics simulation of dynamics-augmented neural objects. *IEEE Robot. Autom. Lett.* 8(5):2780–87
81. Mason MT. 2018. Toward robotic manipulation. *Annu. Rev. Control Robot. Auton. Syst.* 1:1–28
82. Sanchez-Gonzalez A, Heess N, Springenberg JT, Merel J, Riedmiller M, et al. 2018. Graph networks as learnable physics engines for inference and control. In *Proceedings of the 35th International Conference on Machine Learning*, ed. J Dy, A Krause, pp. 4470–79. Proc. Mach. Learn. Res. 80. N.p.: PMLR
83. Battaglia P, Pascanu R, Lai M, Jimenez Rezende D, Kavukcuoglu K. 2016. Interaction networks for learning about objects, relations and physics. In *Advances in Neural Information Processing Systems 29*, ed. D Lee, M Sugiyama, U Luxburg, I Guyon, R Garnett, pp. 4509–17. Red Hook, NY: Curran
84. Allen KR, Guevara TL, Rubanova Y, Stachenfeld K, Sanchez-Gonzalez A, et al. 2023. Graph network simulators can learn discontinuous, rigid contact dynamics. In *Proceedings of the 6th Conference on Robot Learning*, ed. K Liu, D Kulic, J Ichnowski, pp. 1157–67. Proc. Mach. Learn. Res. 205. N.p.: PMLR
85. Zhu X, Wang D, Biza O, Su G, Walters R, Platt R. 2022. Sample efficient grasp learning using equivariant models. In *Robotics: Science and Systems XVIII*, ed. K Hauser, D Shell, S Huang, pap. 71. N.p.: Robot. Sci. Syst. Found.
86. Kim S, Lim B, Lee Y, Park FC. 2023. SE(2)-equivariant pushing dynamics models for tabletop object manipulations. In *Proceedings of the 6th Conference on Robot Learning*, ed. K Liu, D Kulic, J Ichnowski, pp. 427–36. Proc. Mach. Learn. Res. 205. N.p.: PMLR
87. Han J, Huang W, Ma H, Li J, Tenenbaum J, Gan C. 2022. Learning physical dynamics with subequivariant graph neural networks. In *Advances in Neural Information Processing Systems 34*, ed. M Ranzato, A Beygelzimer, Y Dauphin, PS Liang, J Wortman Vaughan, pp. 21910–22. Red Hook, NY: Curran
88. Lee J, Lee J, Bandyopadhyay T, Sentis L. 2023. Sample efficient dynamics learning for symmetrical legged robots: leveraging physics invariance and geometric symmetries. In *2023 IEEE International Conference on Robotics and Automation*, pp. 2995–3001. Piscataway, NJ: IEEE
89. Richards SM, Azizan N, Slotine JJE, Pavone M. 2021. Adaptive-control-oriented meta-learning for nonlinear systems. In *Robotics: Science and Systems XVII*, ed. D Shell, M Toussaint, MA Hsieh, pap. 56. N.p.: Robot. Sci. Syst. Found.
90. Singh S, Richards SM, Sindhwani V, Slotine JJE, Pavone M. 2021. Learning stabilizable nonlinear dynamics with contraction-based regularization. *Int. J. Robot. Res.* 40(10–11):1123–50